JOURNAL OF MATERIALS SCIENCE 22 (1987) 3707–3717

Acoustic emission characterization of flexural loading damage in wood

A. VAUTRIN
Ecole Nationale Supérieure des Mines de St Etienne, 158, cours Fauriel, 42023 St Etienne Cédex, France

B. HARRIS
School of Materials Science, Bath University, Bath BA2 7AY, UK

The paper is concerned with damage accumulation monitored by acoustic emission (AE) techniques during monotonic four-point bending tests on Douglas fir, oak and beech beams. The purpose of the study was to discriminate between the AE responses of the different materials by elementary analysis of ring-down cumulative counting. It appears that this simple method gives results that are species-dependent; in particular, high emission rates were found to be typical of oak samples. The acoustic emission results are related to the observed structural mechanisms of failure of Douglas fir specimens tested in the radial or tangential directions.

1. Introduction

As a consequence of its polymeric nature, wood exhibits viscoelastic characteristics during the early stages of loading. Depending upon the stress level, these may be reversible or non-reversible, and may be studied by such familiar means as dynamic elastic modulus and internal friction measurements. But such methods, being essentially macroscopic, give little or no information about any specific damage mechanisms that contribute to this viscoelastic response. Damage at the level of the cellular structure, which is likely to be species-dependent, will lead, subsequently, to macroscopic damage such as splitting and transverse cracking, and it is of interest therefore to make detailed comparisons of the load–deformation behaviour of different wood species, supporting the mechanical measurements with techniques such as acoustic emission (AE) monitoring and optical microscopy in order to identify species-specific aspects of the development of damage. In this paper we present the results of such a study of the deformation of Douglas fir, oak and beech.

2. Experimental programme and methods

2.1. Materials

The majority of the experiments were carried out on Douglas fir, with smaller quantities of beech and oak being tested. Heartwood, sapwood, and mixed heart–sapwood samples of the fir were available, and in the case of the beech, both normal and reaction wood were tested. Two varieties of oak were examined, the red and pedunculate species. The wood samples were provided as standard beams, 320 mm × 20 mm × 20 mm, by the Station de Recherches sur la Qualité des Bois of the Centre National de la Recherche Forestière (Champenoux, 54280 Seichamps, France).

For the purpose of inter-species comparison the samples tested were all cut in the radial (R) orientation (i.e. with the top and bottom loading surfaces of the beams roughly parallel with the annual rings). Some Douglas fir samples cut in the tangential (T) orientation were also tested. The number of annual rings, which varied little from sample to sample, was about 6 for the fir and 4 for the oak and beech. The moisture content measured on about a dozen separate samples after testing was 10% ± 1%.

2.2. Mechanical testing

The deformation was carried out in four-point bending at a low crosshead speed (0.5 mm min^{-1}) in a 10 tonne screw-driven Instron testing machine. The advantage of the four-point test is that theoretically it induces pure bending in the central portion between the two inner loading points. The only interlaminar shear stresses are induced in the outermost portions of the beam and they can be controlled by increasing the ratio of length L_1 between the inner points to length L_2 between the outer points. When properly conducted, so that both inner loads are the same and compression effects are reduced, the four-point test can be considered as a genuine characterization test, by contrast with the three-point test. The standard values $L_2 = 3L_1 = 270$ mm were chosen for the experiments. Large-diameter (80 mm) loading points were used to minimize compression damage. However, such a precaution results in an enlarged contact area between the loading points and the specimen so that the span-to-depth ratio, i.e. the ratio of L_1 to the thickness h ("height" in terms of a horizontal beam) is less than 4.5. Preliminary tests upon standard beams clearly revealed that compression and shear stresses have a predominant influence on the failure of softwood specimens; furthermore, the contact areas of the loading rollers lead to erroneous estimates of the bending of the beam. In order to avoid compression and shear

0022–2461/87 $03.00 + .12

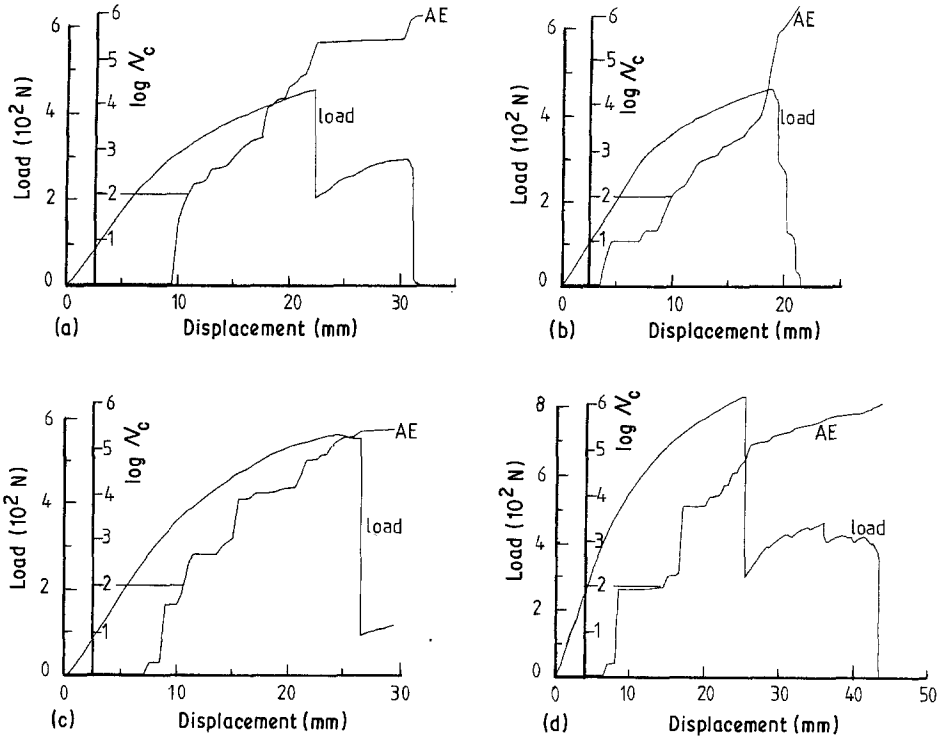

Figure 1 Curves of load and acoustic emission against displacement for (a, b) normal beech and (c, d) pedunculate oak (radial loading).

damage the standard beams were therefore reduced to a thickness of 100 mm instead of 20 mm. It must be emphasised that the span-to-depth ratio (≈ 9) is still very low by comparison with that recommended for glass–epoxy laminates [1]. Nevertheless this thickness appears to be reasonable taking into account the macroscopic heterogeneities of wood (the annual rings). A smaller thickness would increase the experimental scatter because of the difficulty of controlling the effects due to the small misorientations involved in cutting the samples.

2.3. Acoustic emission

AE monitoring was carried out by means of a Dunegan 3000 Series system (Dunegan France SA, Paris) operating with a D-140B PZT transducer (approximate resonant frequency 200 kHz) coupled to the underside (compression face) of the sample in the normal way with silicone grease. The AE signals received by the transducer were preamplified (60dB) and filtered (100 to 300 kHz) by a Dunegan S/D-60P unit, and were subsequently further amplified to 80 or 84 dB, depending on requirements. The counting system used was simple ring-down counting, with a threshold level of 1 V (100 or 63 μV at the transducer depending, again, on the amplification). A full description of the system and its use for the study of fibre composites is given elsewhere [2].

3. Results

3.1. Comparison of hardwoods: beech and oak

In this section we compare the responses of normal beech wood and pedunculate oak tested in four-point bending with radial application of load. Figs 1a to d show the variations, for two specimens of each species, of the load and associated cumulative AE count as a function of displacement of the loading head. There is no particular value in attempting to represent these results in terms of stress and strain using the usual "strength of materials" formula because of the non-linear rheological and structural effects which occur as damage develops. The load–displacement curves for each pair of samples are similar in form up to the first load drop and in all cases are highly non-linear, although the degree of non-linearity for a given level of AE is more marked for the beech. The overall mechanical and acoustic responses for all samples tested are summarized in Tables I and II, for which we have adopted a notional AE threshold of 100 counts (below this level in ring-down counting the actual number of events is too small to be statistically significant). It can be seen that there is practically no acoustic activity below the limit of linear elastic response in the beech, by contrast with the behaviour of oak, the notional AE threshold level being achieved in the beech only at deformations more than double the limit

TABLE I Properties of beech and oak samples

Species	Sample No.	Relative density	Apparent modulus (GPa)	Limit of linearity		
				Strain $\varepsilon \times 10^3$	Stress σ (MPa)	Cumulative AE N_c (counts)
Beech	BNR 261	0.588	12.3	3.85	46.2	0
	BNR 262	0.554	12.6	4.66	58.0	20
Oak	OPR 391	0.714	16.3	4.49	69.0	0
	OPR 392	0.678	16.6	3.66	58.7	0

TABLE II Summary of properties of beech and oak samples at given AE levels

Species	Sample No.	N_c = 100 counts		Point of "failure" (Point A)		
		Strain × 10^3	Stress (MPa)	Strain × 10^3	Stress (MPa)	N_c (10^4 counts)
Beech	BNR 261	8.7	67.0	13	95.3	10
	BNR 262	8.3	67.4	11.8	87.9	12
Oak	OPR 391	6.0	88.0	13.5	130	12
	OPR 392	5.7	64.0	16	138	11

of linear behaviour. It appears, therefore, that neither the first onset of AE nor our notional "threshold" can serve as genuine indicators of the elastic limit of the wood of either species. It can be seen that the AE against displacement curves are more obviously discontinuous for the oak samples than for the beech for which, between threshold and initial failure, there is an approximately linear relationship between log (cumulative AE) and deformation. This distinction correlates with the observation that the deformation of the oak was accompanied by *audible* sounds, implying large bursts of AE in the audible frequency range, whereas no such sounds were heard during the deformation of the beech, in which only the initial rupture was accompanied by audible noise. These audible sounds (in the oak) and the accompanying bursts of AE were found, with the aid of optical microscope observations, to be clearly associated, in the neighbourhood of the maximum load, with the visible rupture of annual rings on the extrados (convex face) of the loaded beams. By contrast, no visible signs of cracking could be seen in the beech up to the point of initial failure. In all cases failure of the samples at maximum load was sudden, with a rapid fall in load level, this drop being accompanied by sudden bursts of AE (although these are sometimes disguised by the logarithmic scales of Figs 1a to d). It can be seen from Tables I and II that the cumulative AE at this point of initial failure is of the order of 10^5 counts for all samples, with relatively little variation despite the fact that the mechanical characteristics and the forms of the individual curves of AE counts against deformation show considerable differences.

Initial failure is precipitated by failure of the first annual ring on the outer face of the beam, this local failure being initiated by tensile fracture of a group of cells followed by a shear failure at the interface between summer growth (latewood) cells and the next layer of spring growth (earlywood). More specifically, the failure appears to be initiated in the first layer of early springwood tracheids [3] (Fig. 2). The propagation of the major shear crack that results from this local failure mechanism is halted in the neighbourhood of the inner roller of the bending jig.

It is noteworthy that the initial rupture of the outer annual ring is not necessarily initiated on the extreme outer surface of the test sample as in the case of a homogeneous material because of the structural and microstructural inhomogeneities of wood. The initial springwood region is particularly susceptible to damage, since the difference in stiffness of the spring and summer wood creates a state of constraint (shear/tension) and on the microstructural scale the tracheids in this region are intrinsically weaker than those which develop at a later stage of growth. It is likely that the damage occurring in this region is a major source of acoustic emission, a suggestion supported by the fact that there is no visible damage on the tensile face (extrados) of a bent beam.

The rapid fracture of the beech visible in Fig. 2 is associated with a certain state of roughness of the failure surfaces on the visible summerwood side of the

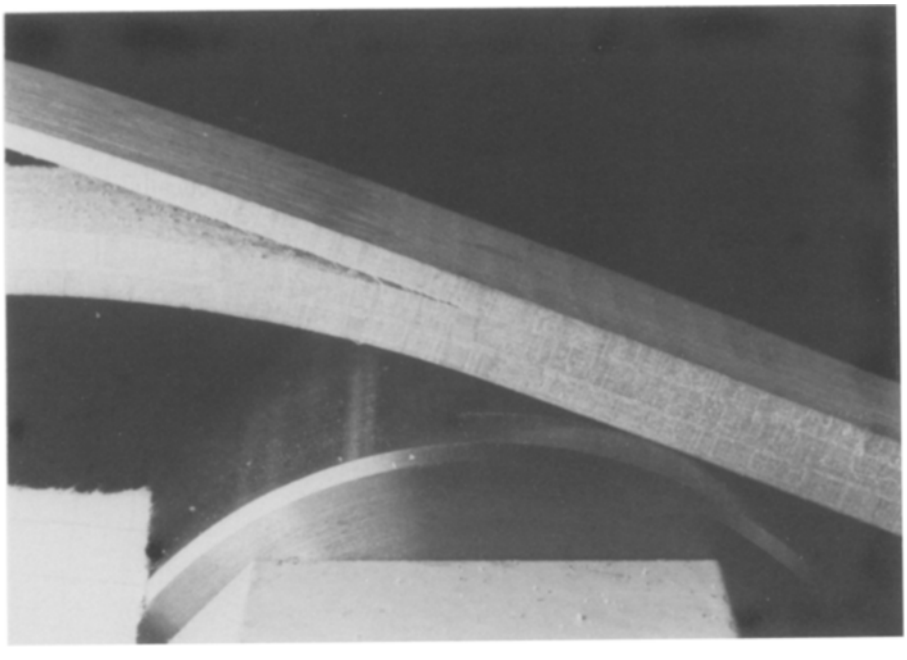

Figure 2 Shear crack at the latewood–earlywood interface in a beech sample.

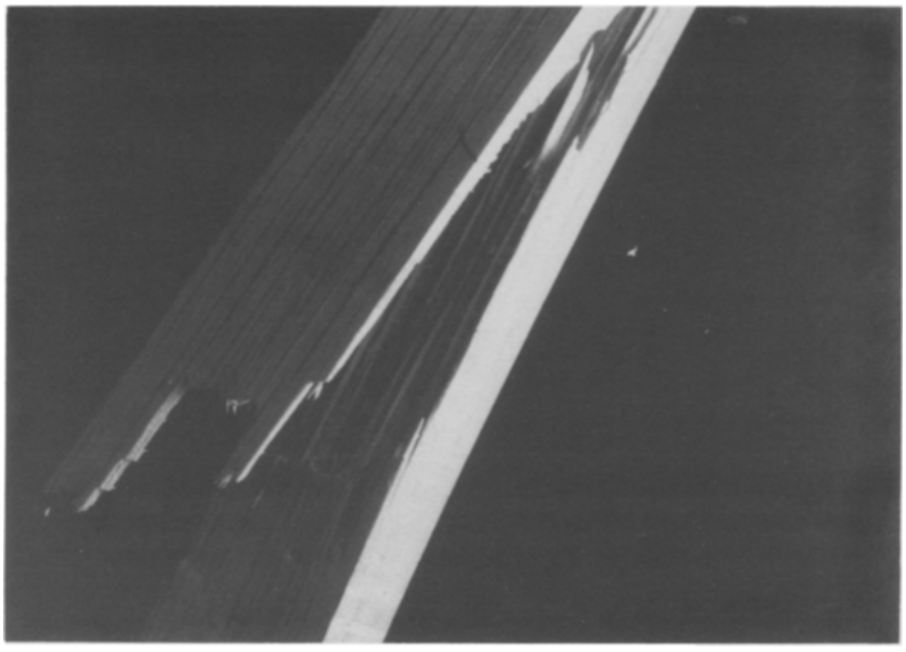

Figure 3 Oblique shear crack through the thickness of an oak sample.

crack (although the crack plane does sometimes cross the annual ring boundaries). The protuberances that are visible in these surfaces are seen under the microscope to be the remains of springwood cell walls with clear indications of shear failure, not unlike the features of interlaminar shear failure in fibre-reinforced plastics.

The failures of oak samples present quite different features. The shear failure surface is not limited to latewood–earlywood interfaces, presumably because of the greater degree of radial uniformity of mechanical characteristics of the oak and a greater degree of microstructural inhomogeneity resulting from the presence of vessels, for example, which leads to a much higher degree of roughness, in a furrowed sense, of the fracture face (Fig. 3). Observation under the microscope confirms the occurrence of oblique shearing of the specimen. The micrograph of the failure surface (Fig. 4) shows tearing of the tracheid walls and shear fracture of the tracheids.

Of all the AE characteristics obtained in this work (including those still to be discussed) only those of the oak samples show any resemblance to curves obtained in earlier work of Ansell and Harris [4] on Scots pine using the same AE equipment as that used in the present study. Samples of this species invariably released acoustic emission in bursts, giving markedly stepped curves like those of Figs 1c and d. In their work they attributed this burst emission to either interlaminar shear in planes of weakness, such as at ray-cell–tracheid interfaces and earlywood–latewood interfaces, or to brittle failure of tracheids. The slower rates of accumulation of AE they ascribed to gradual opening of microflaws as the helically wound cell wall reinforcement gradually extended within the matrix of hemicellulose and lignin.

3.2. Softwood behaviour–Douglas fir

Samples of both sapwood and heartwood were available in Douglas fir, and these have been tested in both radial and tangential orientations. Tables III and IV present mechanical properties and a summary of acoustic emission response for these samples in the same terms as those for beech and oak in Tables I and II.

Figure 4 Failure surface of an oak sample showing shear failure of the tracheids (× 510).

TABLE III Properties of Douglas fir samples

Sample No.*	Relative density	Apparent modulus (GPa)	Limit of linearity		
			Strain, $\varepsilon \times 10^3$	Stress, σ (MPa)	Cumulative AE, N_c (counts)
DSR 181	0.527	17.5	3.80	67.6	500
DSR 182	0.518	19.2	3.75	72.0	750
		15.7	5.71	94.3	300
DST 191	0.514	16.2	3.85	58.6	30
DST 192	0.507	16.9	3.35	52.3	500
DHR 1.1	0.552	19.2	4.39	80.5	500
DHR 1.2	0.557	18.9	3.27	62.8	9050
DHT 2.1	0.518	17.7	3.30	53.6	30
DHT 2.2	0.508	17.6	4.33	67.1	10

*S = sapwood, H = heartwood, T = tangential loading, R = radial loading.

3.2.1. Radial loading (flexure in the L–R plane)

Figs 5a to d show curves of load and AE against deflection for radial loading of two samples each of sapwood and heartwood. The loading curves for these samples are quite different from those for the beech and oak, consisting of a quasi-linear region followed by a relatively flat region with minor perturbations resulting from local fracture events in the tension region of the beam with consequent increases in compliance. These events are again tension/shear failures occurring either in the earlywood or at the latewood–earlywood interface. The values for notional elastic modulus estimated from these curves (Table III) are some 30% higher than values normally reported for this fir [5]. Such a difference could be a consequence of both the size and the macrostructure of the samples. The increase of the span-to-depth ratio from 4.5 to 9 reduces the compression shear damage in the vicinity of the loading points. Previous results were obtained on samples in which only 4 or 5 annual rings were present (for a thickness of 20 mm) whereas 7 or 8 annual rings are present (for a thickness of 10 mm) in our specimens, so reinforcing effects of the latewood in bending could be considerably higher in the latter case. The results are self-consistent, however: the radial stiffness is generally higher than the tangential, and the heartwood stiffness greater than that of the sapwood.

By contrast with beech and oak acoustic emissions at a significant level (and therefore detectable microstructural damage) now occur well within the quasi-linear region of deformation, as shown in Figs 5a to d, even though no corresponding microscopic indication of the damage could be detected. The apparent limit of linear elasticity occurs in general at count levels between 300 and 500 (except in the case of Specimen DHR 1.2). It is not unlikely that the AE detected in this quasi-linear region is associated with compression damage, since the stress levels at the elastic limit are well above the normal values for failure of this species in *longitudinal* compression, although there were, again, no visible signs of compression damage in the appropriate locations. An alternative suggestion is that the emissions are associated with shear rupture of early springwood tracheids even at very low levels of deformation.

The AE curves of Fig. 5 can be crudely divided into three regions. The first is Region I, below the notional "significance" threshold; the second is Region II, from the threshold to the point marked A, where the slope of the AE against displacement curves is markedly reduced; and the third is Region III, beyond Point A to the end of the test. Point A roughly coincides with the beginning of the plateau region of the load–displacement curve, and Region II contains the transition from quasi-linear behaviour to the plateau. In Region II we have regularly observed the gradual development of shear bands, usually oriented at 45° to the specimen axis, on the side faces and in the compression region of the test beams (see Figs 6a and b, for example). The macroscopic shear bands are of course characteristic of shear and compression damage in softwoods, and in the case of our test beams they

TABLE IV Summary of properties of Douglas fir at given AE levels

Sample No.	N_c = 100 counts		Point of "failure" (Point A)		
	Strain $\times 10^3$	Stress (MPa)	Strain $\times 10^3$	Stress (MPa)	N_c (10^4 counts)
DSR 181	3.09	49.3	9.58	117	22
DSR 182	1.30	19.4			
	5.67	88.7	10.4	112	12.5
DST 191	5.13	76.4	6.60	90	1.25
DST 192	2.72	42.8	5.30	75	0.95
DHR 1.1	3.08	54.6	8.57	122	2.70
DHR 1.2	1.22	21	6.80	102	14.7
DHT 2.1	3.29	51.6	8.57	103	1.08
DHT 2.2	6.18	94	7.00	100	1.16

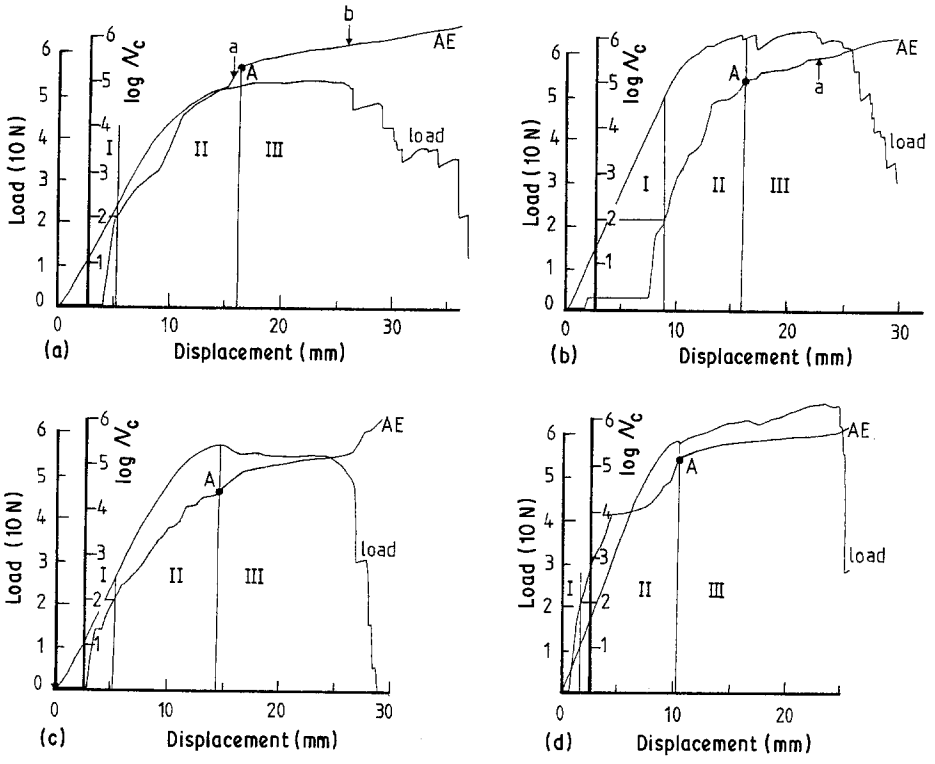

Figure 5 Load and AE against displacement curves for Douglas fir: (a, b) sapwood, (c, d) heartwood (radial loading).

indicate a displacement of the neutral axis of the beam towards the tension face. Simultaneously, very limited zones of damage in tension become visible towards the end of Region II. As a load-bearing material the wood is therefore clearly ruined before Point A is reached, even if uncrushed.

The transition from quasi-linear to highly non-linear behaviour in Region II is not marked by any significant change in the general form of the log (AE) against displacement curve. Monitoring of the rate of emission does not therefore permit us to distinguish any differences in damage mechanism operating in these two stages of quite distinctive mechanical response within Region II. It is not known at this stage whether amplitude analysis could provide a means of identifying changes of mechanism. Thus, although AE ring-down counting results correlate reasonably well with mechanical response in the sense that Point A, which corresponds to a marked change in the AE characteristic, also coincides with a point of irremedial damage in the wood, it is nevertheless not a technique that can identify the more critical onset of impairment of load-bearing ability that coincides with the end of quasi-linear response (prior to the development of shear zones).

The stresses and strains at Point A can have no value other than a comparative one, since they lie outside the range of linear behaviour for which "strength of materials" calculations are valid. Beyond this point, a multiplicity of simultaneous damage mechanisms occurs, the combined compression/shear mode continues to develop, and tension/shear failures begin to establish themselves (Fig. 6c). These involve sudden drops in load (rigidity) associated with significant changes in the range of acoustic emission. Visual observation confirms that tensile failure is initiated by failure of tracheids on the extrados – a region in which there is an inevitable sensitivity to the presence of imperfections – and it develops substantially transversely in the springwood. The micrograph of Fig. 7a clearly shows the two different failue mechanisms occurring in the region in tension:

(i) on the right side: failure in tension of the springwood tracheids on the extrados, and

(ii) on the left side: the failure in tension is stopped at the latewood–earlywood interface and shear rupture of the cell wall of the first springwood tracheids occurs and subsequently propagates.

Parts of torn cell walls and helical thickenings can be observed in the springwood rupture surface (Fig. 7b), revealing that the helical thickenings have a mechanical reinforcement.

3.2.2. Tangential loading (flexure in the L–T plane)

Unlike the situation in radial loading, the load–displacement curves for tangential loading depend on whether the wood is heartwood or sapwood (Figs 8a to d). Although the initial stages of the curves (Regions I and II) are identical, the final rupture of heartwood, identified by our Point A, begins at a deformation of about 16%, by comparison with about 12% for the sapwood. In this mode of loading, the mechanisms of failure of the two types of wood are also well differentiated, presumably because of the reinforcing role of the summerwood, the strength of which is significantly higher in the heartwood. The initial parts of the tangential loading curves are noticeably non-linear, unlike those for radial loading, and the apparent elastic moduli recorded in Table III are tangent moduli estimated at the point of inflection. This non-linearity is likely to be a result of local compression damage. The plateau region of the load–

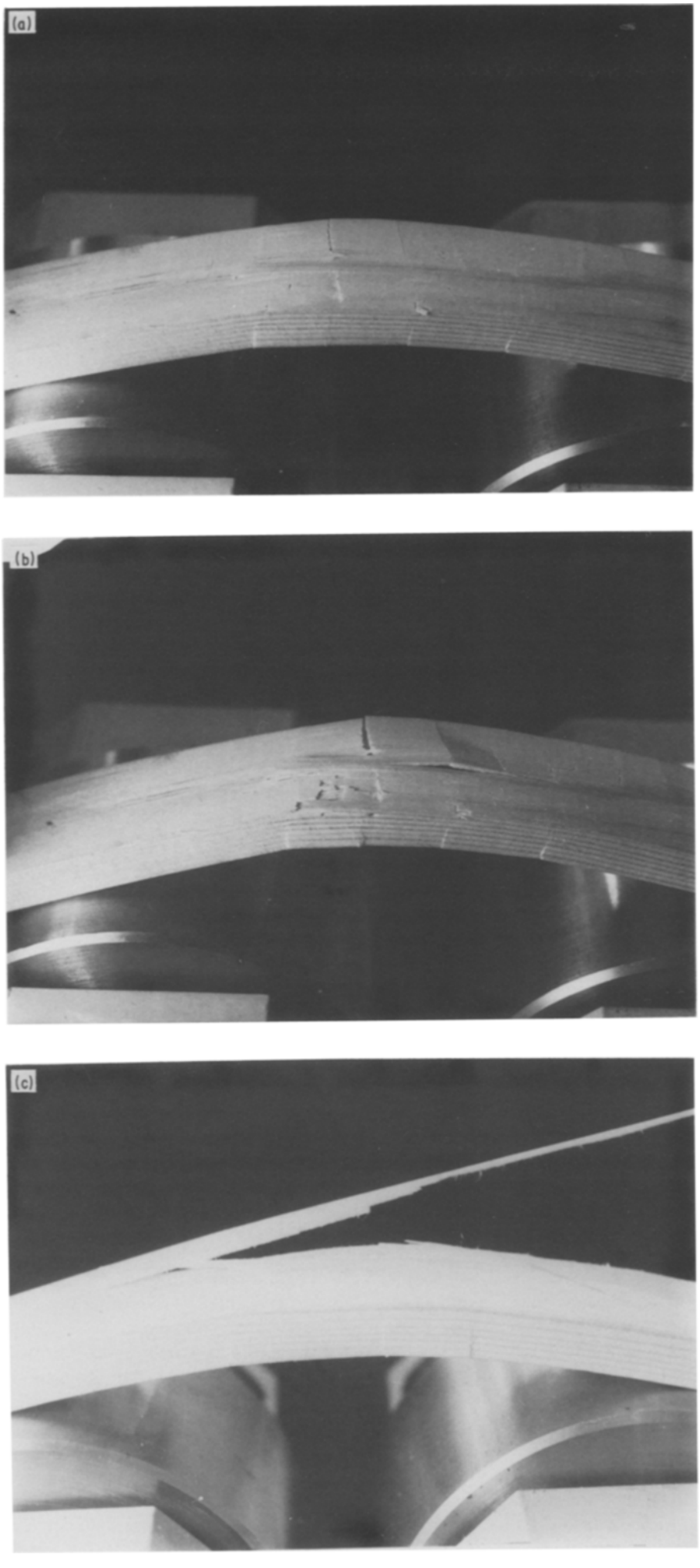

Figure 6 (a) Ruin in compression of a Douglas fir sapwood sample; the two components of the shear are clearly visible, (Point "a" on Fig. 5a). (b) Development of damage in compression/tension failure of the first annual ring and shear cracking of a Douglas fir sample (Point "b" on Fig. 5a). (c) Propagation of a shear crack through the latewood–earlywood interface and damage in compression of a Douglas fir sample (Point "a" on Fig. 5a).

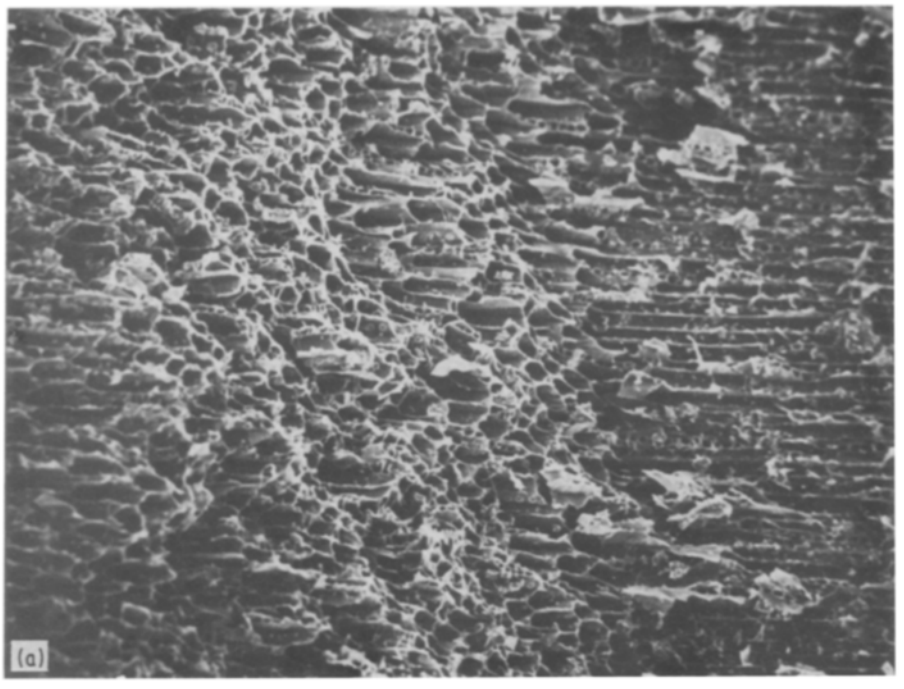

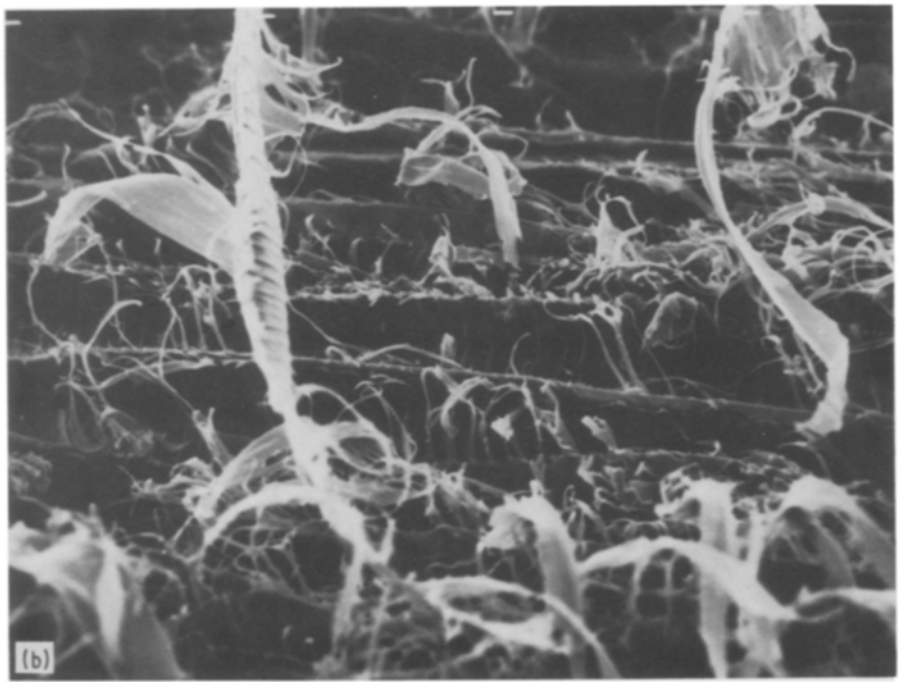

Figure 7 (a) Failure surface of a Douglas fir sample in radial loading; view of the tensile failure of the softwood tracheids and the latewood surface (×55). (b) Failure surface of a Douglas fir sample in radial loading; view of softwood surface (×260).

deformation curves for heartwood samples is relatively poorly defined by comparison with the radial loading curves, and there is no plateau region at all in sapwood samples.

There are, furthermore, no indications of compression damage in tangential loading, in strong contrast to the response in radial loading. As expected, the apparent stiffness of the sapwood is lower than that of the heartwood (Table III), although the maximum stresses are of the same order, regardless of the mode of loading. Failure in the sapwood samples is seen to be catastrophic (rupture by oblique shear through the specimen) (Figs 8a, 8b and 9) whereas in the heartwood it is controlled (cracking of earlywood), as shown in Figs 8c, 8d and 10.

AE rates were higher and more discontinuous in tangential than in radial loading, with the result that there is a greater spread of characteristic values of stress levels at the nominal AE threshold of 100 counts during tangential deformation (Table IV), and this point is found to be situated in the non-linear region of the load–deflection curves. The strain (or stress) levels for critical damage (Point A) are found to be much lower for sapwood than for heartwood, although, surprisingly, the overall numbers of counts are similar and of order 10^4 to 10^5 (Table IV). No other (visible) sign of damage is observed at this point.

The curves of AE against deformation exhibit two distinct regions. After an initial period without emission, AE begins at a high rate in a discontinuous manner, the steps in the AE curves being accompanied by audible sounds. This first region is then followed by a second, characterized by a lower and fairly constant rate of emission, the transition between the two regions again being well defined. We may define this as Point A, but by contrast with the case for radial

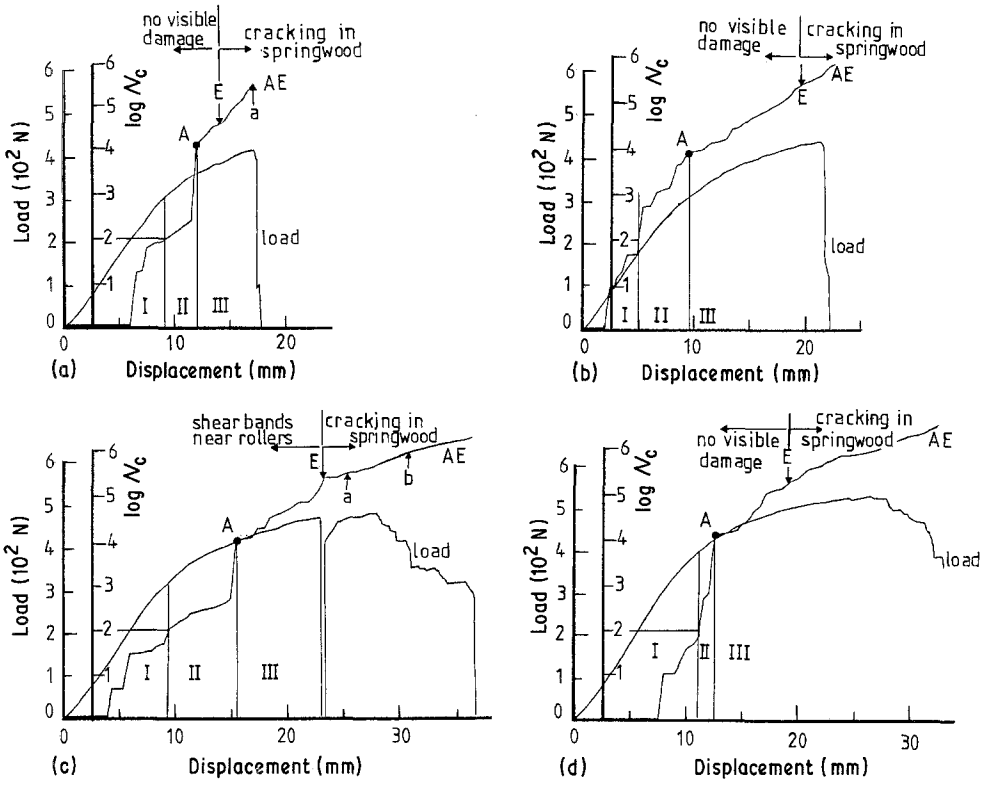

Figure 8 Load and AE against displacement curves for Douglas fir: (a, b) sapwood, (c, d) heartwood (tangential loading).

loading, there is no other indication of changing structure or damage at this point. Visible signs of structural damage occur only at deformations much higher than this (Point E in Figs 8a to d) in Region III of the deformation. These indications consist of macroscopic transverse fissures in the initial springwood under tensile load, but there are no signs of lateral shear or compression damage by the end of Region II, no matter what the nature of the lateral faces of the sample. Some shear bands were also visible on the compression (unobserved) faces of the beams after test.

Although the cracking of the springwood again appears to start at the latewood–earlywood interface, no visible evidence of the macroscopic rupture of this interface could be found until a very advanced stage of cracking. This invites a study of the fracture process at much higher levels of magnification. Initiation of cracking at the latewood–earlywood interface, followed by transverse cracking across the earlywood, is clearly shown in Fig. 10a. Subsequently, L–T shear failure of the interfacial region occurs (Fig. 10b).

4. Conclusion

Acoustic emission monitoring permits the establishment of criteria for critical levels of damage, visible or non-visible, in deformed wood samples. At the simple level of event or ring-down counting, however, the AE characteristics do not appear to be able to give generally useful and "generalizable" means of establishing

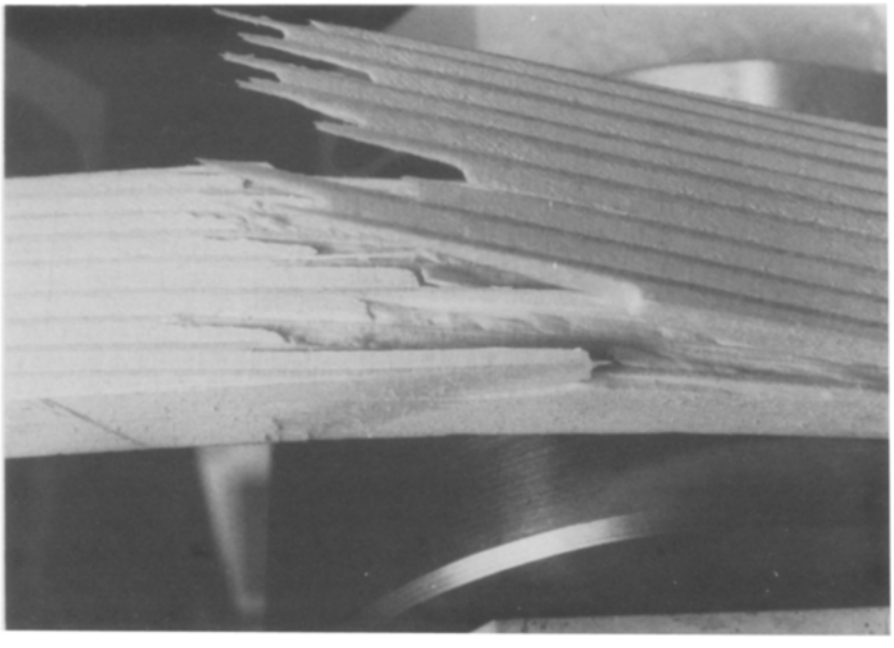

Figure 9 Oblique shear crack through the thickness for Douglas fir sapwood (Point "a" on Fig. 8a).

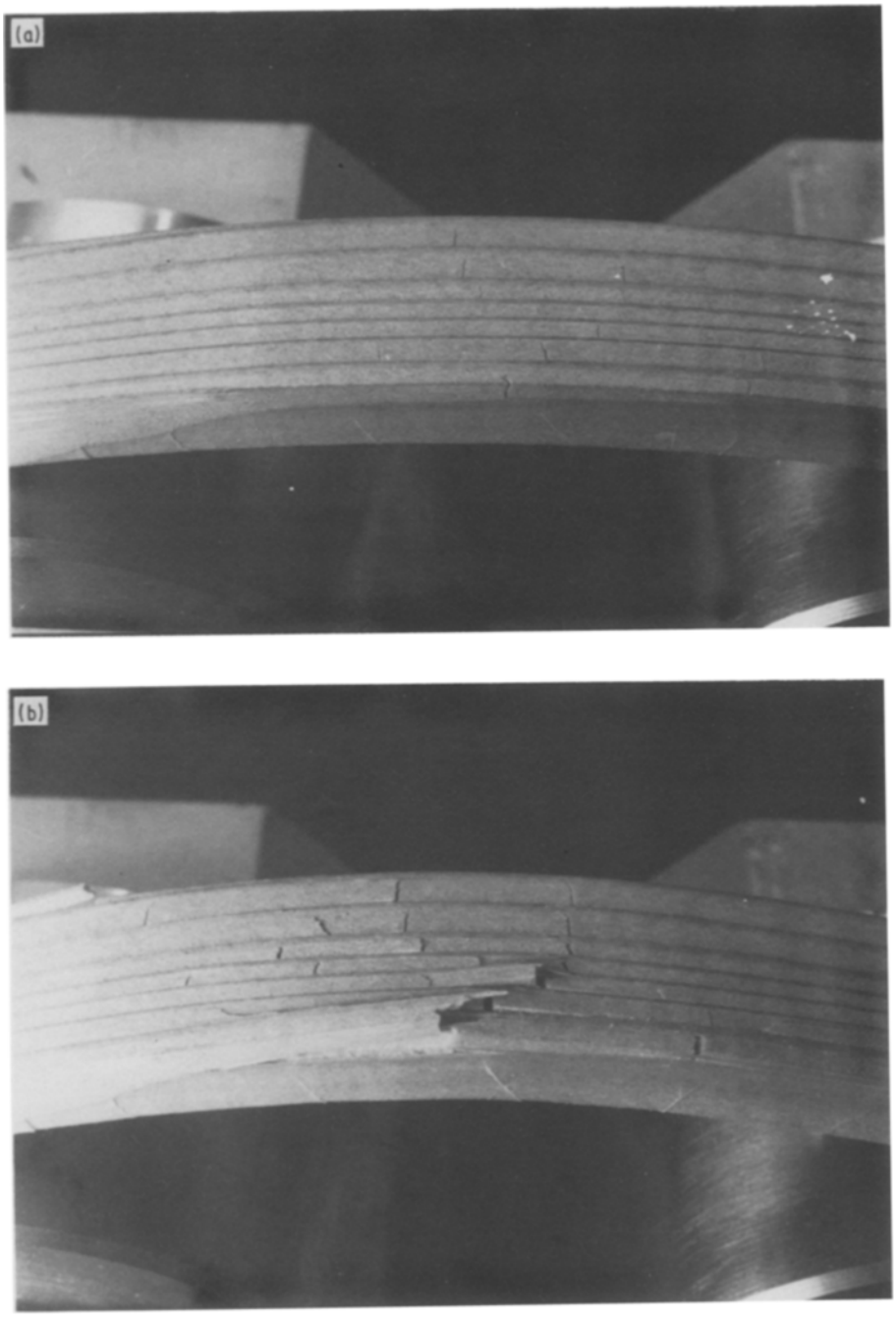

Figure 10 (a) Transverse cracks in earlywood for Douglas fir heartwood; starting point is the latewood–earlywood interface (Point "a" on Fig. 8c). (b) Some latewood–earlywood interfaces are broken, but the latewood stops the transverse cracks which grow through the earlywood in Douglas fir heartwood (Point "b" on Fig. 8c).

damage levels that are clearly related to microstructural mechanisms of ruin, since the AE response appears to be dependent on both the species and the loading mode.

The AE indications of serious damage frequently do not coincide with mechanical parameters derived from conventional macroscopic loading tests.

Acknowledgements

The authors wish to thank the Station de Recherches sur la Qualité des Bois of the CNRF for providing the specimens. A. Vautrin is grateful to Mr H. Polge, Head of the Station, for scientific advice and encouragement.

References

1. C. B. BERT, in "Composite Materials", Vol. 8, Structural Design and Analysis, Part II, edited by C. C. Chamis (Academic, New York, 1975) pp. 73–133.
2. B. HARRIS, F. J. GUILD and C. R. BROWN, *J. Phys. D: Appl. Phys.* **12** (1979) 1385.
3. R. E. MARK, "Cell Wall Mechanics of Tracheids" (Yale University Press, New Haven, Connecticut, 1967).
4. M. P. ANSELL and B. HARRIS, in Proceedings of 3rd International Conference on Mechanical Properties of Materials, August, 1979 (ICM3), Cambridge, Vol. 3 (Pergamon, Oxford, 1979) pp. 309–318.
5. J. BODIG and B. A. JAYNE, "Mechanics of Wood and Wood Composites" (Van Nostrand Reinhold, New York, 1982).

Received 4 December 1986
and accepted 28 January 1987